Iraqi journal of civil engineering (IJCE)
P-ISSN: 1992-7428 ; E-ISSN: 2706-686X
Vol. 18 , No. 2 (2024) , pp. 1 ~ 14
DOI: 10.37650/ijce.2024.180201

Iraqi Journal of Civil Engineering

Journal homepage: https://ijce.uoanbar.edu.iq/

Construction of The Load-Transfer Curves for Piles in Sand as a Function of The Standard Penetration Test

Ali Bouafia[a*], *Abdesselem Laouedj*[b]

[a]*Department of Civil Engineering, Faculty of Technology, University of Blida1, Blida, Algeria,*

[b]*National School of Marine Science and Coastal Planning, Algiers, Algeria*

PAPER INFO

Paper history
Received: 09/05/2024
Revised: 23/06/2024
Accepted: 08/07/2024

Keywords:
Piles
Loading test
P-Y curves
Sand
Settlement

Copyright: ©2024 by the authors. Submitted for possible open-access publication under the terms and conditions of the Creative Commons Attribution (CC BY-NC 4.0) license.
https://creativecommons.org/licenses/by-nc/4.0/

ABSTRACT

In this paper, a practical method of analysis of pile displacements is proposed based on the theory of load-transfer curves widely used in pile design and analysis. The parameters of the load-transfer curves for piles under axial load (called t-z, q-z curves) and lateral load (called P-Y curves) were correlated with the number of blows N_{spt} measured during the standard penetration test (SPT). Well-documented case histories of full-scale axial or lateral loading tests on single piles in sand were collected, and the analysis of the experimental results led to define the parameters of the load-transfer curves. Two practical computation methods of a single pile under an axial or a lateral load were proposed to be used within the scope of a pile foundation project. Finally, a validation process of the load-transfer curves was undertaken by directly comparing the predicted pile displacements to those measured during other pile loading tests, showing good predictive capability for the two proposed methods.

1. Introduction

The pile foundation design based on limit states concept usually requires to check the ultimate limit states (ULS) as well as the serviceability limit state (SLS). The first one necessitates the determination of the pile bearing capacity Q_l under an axial load and/or the pile lateral resistance under a lateral load. The second one necessitates an analysis of the pile displacements. More precisely, the pile settlement under an axial load and/or the pile deflection under a lateral load should be within the permissible values prescribed by the structure. Pile displacements may be determined by measurements during a pile loading test, or estimated by computation on the basis of commonly used methods like the analytical elasticity methods, the numerical methods, and the load-transfer methods (Poulos & Davies, 1980; Briaud, 2023). The last category of methods is widely used in pile design because of the simplicity of modelling of the pile/soil interaction and relatively simple equations to be used. The concept of load-transfer consists in replacing the pile/soil interface by a series of nonlinear springs following an elastic-plastic constitutive law.

As depicted in Fig. 1, the load-transfer curves describing the pile/soil interface response to an axial load, are

* *Corresponding author.*E-mail address: ali.bouafia@univ-blida.dz

the τ-v curve (τ: skin friction stress, v: pile settlement), defined by the friction stiffness B_0 and the limit skin friction stress q_s, and the q_p-v_p/B curve (q_p: vertical pressure at pile tip, v_p :Pile tip settlement, B: Pile diameter), defined by the pile tip modulus R_0 and the end bearing capacity q_l (Mosher & Dawkins, 2000). Under very small values of Q, the curves may be assumed to be linear shaped, which implies that:

$$\tau(z) = B_0(z).y(z) \quad (1)$$

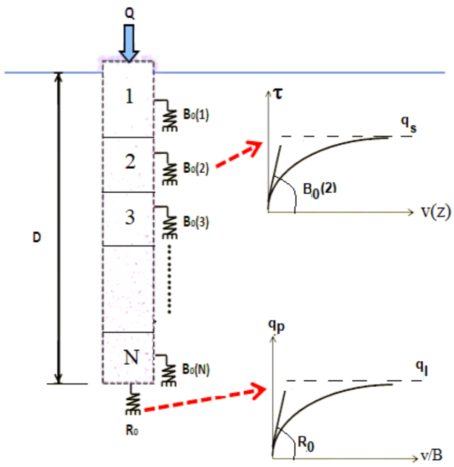

Fig. 1 Scheme of load-transfer of an axially loaded pile

$$q_p = R_0\left(\frac{v_p}{B}\right) \quad (2)$$

The governing equation to compute the pile settlement *v(z)* is (E_p: Pile Young's modulus):

$$\frac{d^2v}{dz^2} - 4\frac{B_0}{E_pB}v = 0 \quad (3)$$

In practice, this equation is numerically solved by using usual software requiring the input of the load-transfer curves. According to Fig. 2, the pile/soil interface response under a lateral load is described by the P-Y curves. At a given depth z, this curve is defined, as shown in Fig. 3, by the lateral reaction modulus E_{s0} and the lateral soil resistance P_u.

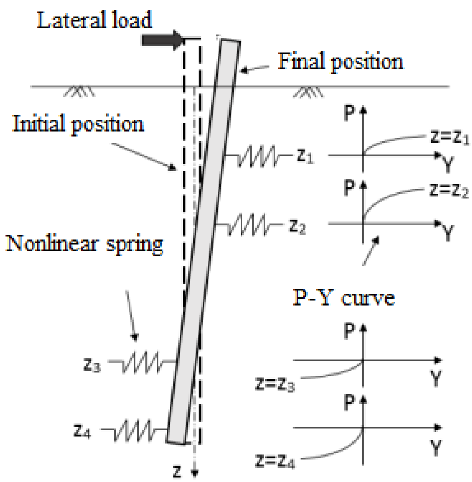

Fig. 2 Scheme of load-transfer of a laterally loaded pile

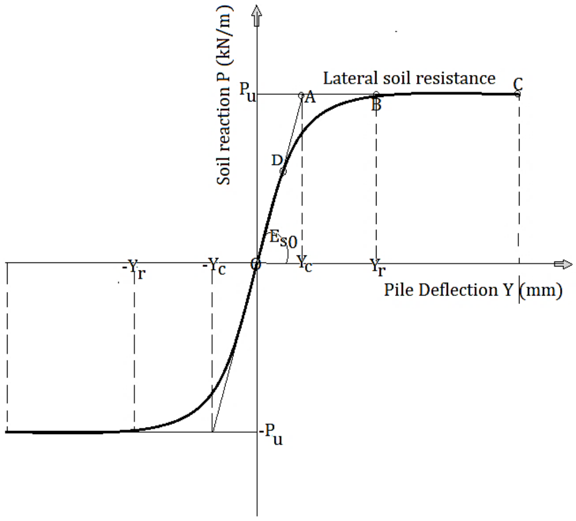

Fig. 3 Scheme of P-Y curve at a given depth

Under very small values of the lateral load H, the P-Y curve may be approximated to the linear portion OA, as illustrated in Fig. 3, which may be expressed as:

$$\boldsymbol{P(z) = E_{s0}(z).Y(z)} \tag{4}$$

The pile deflection Y(z) may be computed based on the fundamental equation of a beam on an elastic foundation, as follows:

$$\boldsymbol{E_p I_p \frac{d^4Y}{dz^4} + E_{s0}(z).Y(z) = 0} \tag{5}$$

Similarly, a practical numerical solution of this equation is obtained by introducing the P-Y curves as input data in some usual software of pile foundation design. However, the main difficulty in such a computational approach is the direct estimation of the parameters B_0, R_0, q_s, q_l, E_{s0}, and P_u from the geotechnical properties, particularly the standard penetration test (SPT). To the knowledge of the authors, many studies were undertaken to directly correlate these parameters to some in-situ test data, namely the pressure meter test (PMT) (Ménard et al., 1971; Baguelin et al., 1978; Frank & Zhao, 1982; Bouafia, 2007; Bouafia, 2023a) and the cone penetration test (CPT) (Verbrugge, 1981; AFNOR, 2012; Bouafia, 2023b), but there is seemingly a very few published works on the contribution of the SPT test to a direct evaluation of the parameters of load-transfer curves for piles. The indirect estimation of these parameters is usual in the current practice, although it is unsatisfactory because it leads to non-negligible uncertainties in such correlations. For example, by using the API (American Petroleum Institute) method to build the P-Y curve, E_{s0} and P_u may be estimated as from the angle of internal friction, this latter being correlated to the N_{spt}.

The present paper aims to present the results of an important research work undertaken at the University of Blida1, which contributes to a practical definition the parameters of hyperbolic load-deflection curves for single piles in sand in correlation with the N_{spt} measured during the SPT. After a brief description of the experimental data collected from several full-scale loading tests on piles, the methodology of analysis is outlined and the results are discussed.

2. Load-transfer curves for piles under axial loads

2.1. Description of the experimental sites

The collected data includes 50 load tests on bored piles at 27 sites located in the United Arab Emirates. As illustrated in Fig. 4, all the sites are located along the coast of the Arabian Gulf, specifically in Dubai, Sharjah, and Ajman, areas experiencing rapid infrastructure development.

The soil stratigraphy studied in this database consists of layers of fine to medium dune sand, slightly silty or silty with traces of gravel, gypsum, shell fragments, or cemented sand. At significant depths, horizon of soft rocks such as sandstone or calcarenite are usually detected, and characterized by unconfined compressive strengths ranging from 0.4 to 5 MPa.

The groundwater table typically fluctuates near the surface of the soil, and the characterization of sandy soil is usually undertaken by using the Standard Penetration Test (SPT), which, is the most commonly used in-situ test in this country. Although there is some equipment diversity, the typical apparatus features are a 63.5 kg hammer with a free fall of 76 cm. The split-spoon sampler has a length of 75 mm and an internal diameter of 35 mm. The measured blow count N_{spt} at the base of the studied piles varies between 42 and 100, corresponding to dense to very dense sand.

The piles included in this database were bored in a sandy horizon with casing or mud rotary drilling, commonly using the bentonite. The pile tips are far form from the rock layer, and their diameters and slenderness ratios vary in margins of 0.5-1.1 m and 10.7-34 respectively.

Static vertical loading test is often conducted following the ASTM D 1143-81 standard (ASTM, 1994). Typically, the test is performed on piles that are simply instrumented at the top with four dial gauges to measure the settlement v_0, and the vertical load Q is incrementally applied using a hydraulic jack in contact with beams. These beams are loaded either by counterweights or in connection with anchor piles.

The loading test program generally consists of 2 one-way loading cycles, with increments of 25% of the maximum load for each cycle. The first and second cycles have maximum loads corresponding to the calculated design load and 1.5 to 2 times the maximum design load, respectively. Each increment is maintained until the settlement rate falls below 0.25 mm/hour, without exceeding 2 hours for each increment (Bouafia & Derbala, 2002; Bouafia, 2023c).

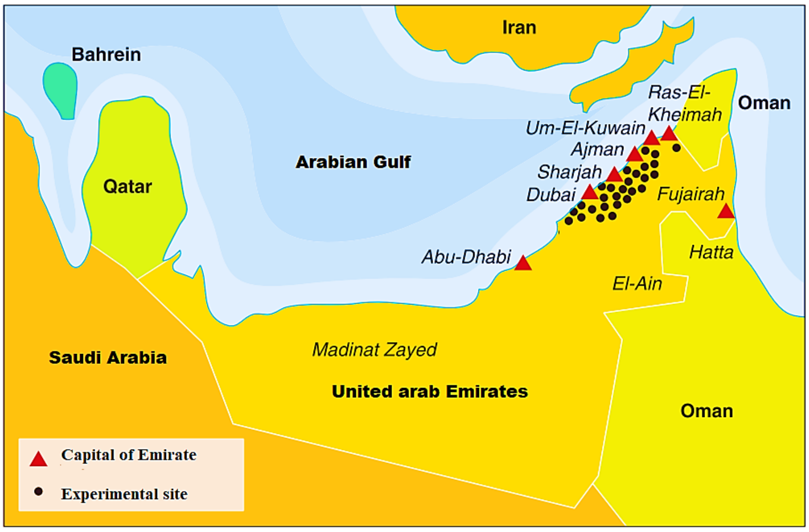

Fig. 4 Map of the experimental sites of vertical loading tests

2.2. Methodology of analysis

A pragmatic approach, attempting to circumvent the uncertainties of a theoretical pile/soil interaction model, may be undertaken based on the back-analysis of a database of full-scale pile loading tests, by correlating the parameters of load-transfer curves, namely B_0, R_0, q_s, and q_l to the number of blows N_{spt}, according to the following equations:

$$q_l = K_{N1}.N_{spt}^{eq} \quad (6)$$

$$q_s = K_s.N_{spt} \quad (7)$$

$$R_0 = E_{E1}.N_{spt}^{e} \quad (8)$$

$$B_0 = K_{E2}.\frac{N_{spt}}{B} \quad (9)$$

K_{N1} and K_s are respectively the end bearing capacity and the limit shaft friction factors, and K_{E1} and K_{E2} are respectively the modulus numbers at the pile tip and along the pile shaft. All these factors have the dimension of a stress (kPa or MPa).

As depicted in Fig. 1, the τ-v curve may be formulated as a hyperbolic function as follows:

$$\boldsymbol{\tau = \frac{v}{\frac{v}{q_s}+\frac{1}{B_0}}} \quad \textbf{(10)}$$

Similarly, the q_p-v_p curve is described by a hyperbolic function:

$$\boldsymbol{q_p = \frac{v_p}{\frac{v_p}{q_l}+\frac{B}{R_0}}} \quad \textbf{(11)}$$

Based on the analysis of instrumented pile loading tests database, Briaud and Tucker (1984) proposed hyperbolic load-transfer curves for piles in sand, where the friction stiffness B_0 and the pile tip modulus R_0 (expressed respectively in MPa/m and MPa) are correlated to the measured blow count N_{spt} as follows:

$$\boldsymbol{B_0 = 21.16(N_{spt})^{0.27}} \quad \textbf{(12)}$$

$$\boldsymbol{R_0 = 50.12(N_{spt}^m)^{0.0065}} \quad \textbf{(13)}$$

N_{spt}^m is an arithmetic average of the measured values, considering a thickness zone of 4*B* below the pile tip and 4*B* above it.

It is remarkable from equation (12) that B_0 does not take into account a possible diameter effect, as expected by equation (9). Moreover, according to equation (13), R_0 slightly depend on the soil density. In fact, for a margin 10-50 of N_{spt} corresponding to a wide range of density from very loose sand to very dense sand, R_0 is practically equal to 51 MPa, which is in contrast with the fundamental fact that the pile/soil stiffness increases with the soil density.

In a similar approach of analysis, Horiuchi and Kani (1998) studied a database of 18 pile loading tests on precast concrete bored piles in very dense sandy soils and suggested a margin of 0.6-2.0 MPa/m for the ratio R_0/B for small diameter piles (margin of diameter=0.35-0.8 m) with embedded lengths varying between 12 and 67 m, the modulus R_0 was defined as corresponding to a settlement of 2% of B. At this level of pile settlement, it corresponds to a rather secant stiffness, whereas R_0 should correspond to a very small level of pile settlement. This latter was found to be up to 0.3% of B for reinforced concrete bored piles in sandy sands (Bouafia, 2023c).

In the present study, a back-analysis was undertaken to simulate the experimental load-settlement curve at the pile top, by gradually varying the values of $B_0(z)$ and R_0, as well as $q_s(z)$ and q_l, until the calculated curve satisfactorily fits the experimental curve, which requires, according to the technique of least squares fitting, a value of the coefficient of regression R close to 100%. Fig. 5 illustrates an example of calibrating the calculated curve by back-analysis of the experimental curve obtained during a loading test. For all the test piles, R was found varying between 70% and 99%.

The software SETPIL (SETlement of PILes), developed at the University of Blida**,** and based on the hyperbolic load-transfer curves to simulate the load-settlement curve, was used as a computational tool for such a task (Yaich-Achour, 2004).

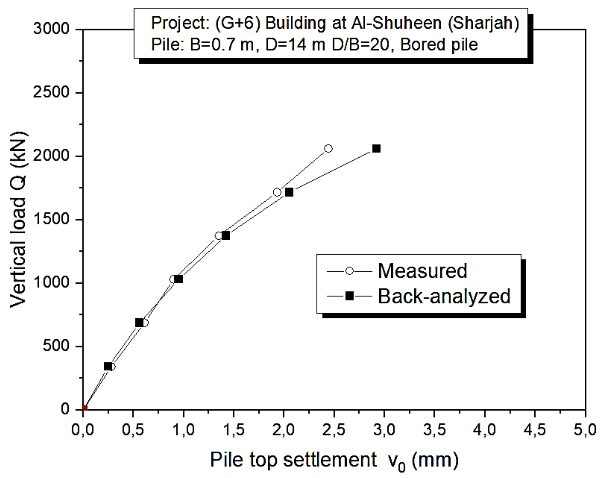

Fig. 5 Example of a calibration of load-settlement curve

2.3. Presentation and discussion of results

A synthesis of the results of the back-analysis of all the test piles led to propose the following values:

$$K_{N1} = 120kPa \tag{14}$$

$$K_s = 4.1kPa \tag{15}$$

$$K_{E1} = 17.5MPa \tag{16}$$

$$K_{E2} = 4MPa \tag{17}$$

It is to be noted that the N_{spt}^{eq} expressed in equation (6) was conventionally defined as an arithmetic average value along 3B below the pile tip and 8B above it (Bowles, 1977).

The term N_{spt}^{e} appearing in equation (8) was defined as the weighted average value along 2B below the pile tip, as per the following conventional equation:

$$N_{spt}^{e} = \frac{1}{2B}\int_{D}^{D+2B} N_{spt}dz \tag{18}$$

To take account of a possible absorption of the driving energy during the SPT test in fine sands or silty sands below the water table, the recommendation of PHRI (1980) was adopted by correcting the N_{spt} measured value exceeding 15 as follows:

$$N_{spt}^{c} = 15 + \frac{N_{spt}^{m} - 15}{2} \tag{19}$$

N_{spt}^{m} and N_{spt}^{c} are respectively the measured and the corrected values at a given depth below the ground.

Moreover, in accordance with several geotechnical standards (CGS, 2006; AFNOR, 1992), q_s should be bounded, for safety considerations, to 120 kPa for bored piles (simple drilling or mud drilling) in sandy soils.

2.4. Validation of the proposed method

The predictive capability of the proposed hyperbolic load-transfer curves for bored piles in sand was assessed through the prediction of the load-settlement of piles in 7 well-documented case histories of loading tests carried out in 4 sandy sites.

In El-Mohammadia, Algiers, two loading tests were conducted on reinforced concrete piles. The first pile (PV3) has a diameter of 1 m and a length of 20 meters (D/B=20). The second pile (PV5) has also a diameter of 1 m and a length of 23 m (D/B=23). Both piles were installed in a horizon composed of fine sand with a transition zone containing rolled aggregates including sand, gravel, and stones. The water table was detected at depths of 8.5 m and 11.2 m below the surface for PV3 and PV5, respectively. The Young's modulus of the reinforced concrete was estimated to be 32000 MPa.

In Taipao, Taiwan, a reinforced concrete pile (B9) with a diameter of 1.5 m and an embedded length of 34.9 m, was bored by mud drilling in a soil composed of alternating layers of silty sand (SM) and slightly plastic silt (ML). The water table was detected at a depth of 1 m below the surface (Huang et al., 2001).

At an experimental site in Sao-Carlos, Brazil, das Neves et al (2001) conducted vertical loading tests on three piles. These piles had the same length of 10 m and three different diameters: 0.35, 0.40, and 0.50 m. The Young's modulus of the reinforced concrete was estimated to be 32000 MPa. These piles were bored by dry drilling in a soil composed of clayey sand (SC), with a water table detected at a depth of 11 m below the surface (das Neves et al., 2001).

Within the framework of a prediction event of the vertical pile response, organized during the DFI conference (Deep Foundations Institute), in May 2014, a full-scale pile loading test was conducted in Santa-Cruz, Bolivia (Fellenius, 2014). The test pile (TP1) is a reinforced concrete pile, with a diameter of 0.44 m, an embedded length D of 17.5 m, bored with mud drilling. The soil layers are a dense to very dense, fine to medium grained sand, containing traces of fines and submerged by a ground water detected at 2.5 m of depth.

The load-settlement behavior of each test pile was simulated by using the proposed load-transfer curves, which were input in the software SETPIL. Each pile test was subdivided into thin segments, and the hyperbolic load transfer curves were defined at the mid-point of each segment. The parameters B_0, R_0, q_s and q_l were determined using equations (6)-(9) and (14)-(17).

As an illustrative example, Fig. 6 illustrates the load-displacement curve for pile PV3, showing an excellent agreement between predicted and measured settlements up to a load of 9000 kN.

As shown in Fig. 7, considering the ratio computed settlement to measured settlement as a random variable within a population of 64 values, led to build its histogram which fits well with a Gaussian probability distribution, with a mean μ equal to 0.85 and a standard deviation σ of 1.143. To the value of μ corresponds an estimated probability of 70%, and a confidence interval of 0.76-0.93 for a confidence level of 95%. This result is encouraging, seeing the multitude of assumptions and uncertainties during the step of back-computation approach used to define the load-transfer curves.

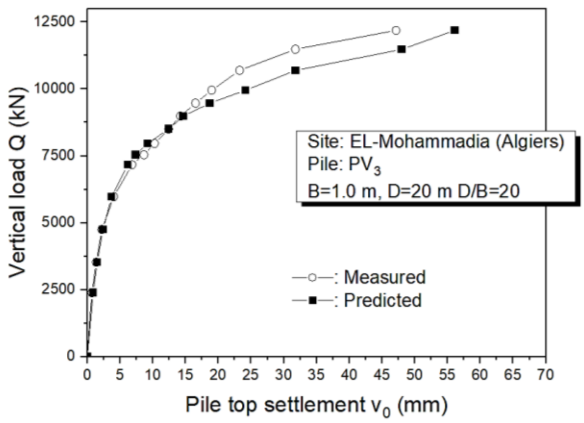

Fig. 6 Comparison between predicted and measured load-settlement curves

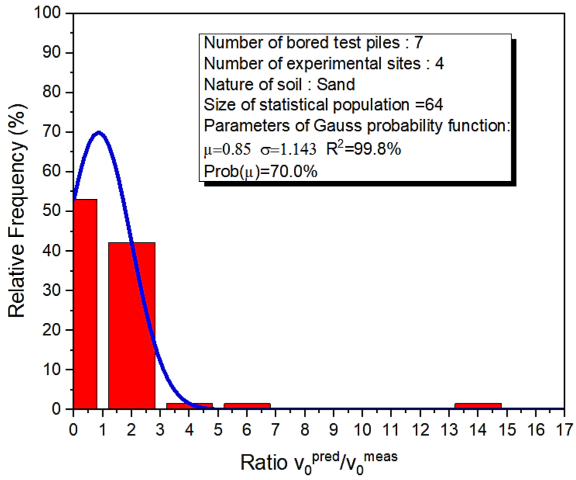

Fig. 7 Histogram of the ratio predicted to measured settlement

3. LOAD-transfer curves for piles under lateral loads

3.1. Description of the experimental sites

15 well-documented case histories of full-scale lateral loading test of single piles carried out in 9 sandy sites worldwide were collected and analysed. Selection of the case studies was based on the instrumentation of the test pile, which allows measuring the bending moment profiles and hence deriving the experimental P-Y curves. The instrumentation adopted was the strain gauges, linear potentiometers, and the tiltmeters.

As summarized in Table 1, the diameter (or width) and the slenderness ratio vary within the margins 0.3-1.2 m and 10-40 respectively.

3.2. Methodology of analysis

The P-Y curves for full-scale instrumented piles under lateral loading tests may be determined following three steps:

1. Determination of the profiles of moment M(z) and fitting them by an analytical function like a polynomial function or a spline function.
2. Double integration of the fitting function of the bending moment profile M(z) to determine the deflection Y(z) as follows:

$$\boldsymbol{Y(z) = \frac{1}{E_p I_p}\int(\int M(z)dz)dz + Y'_0 z + Y_0} \quad \textbf{(20)}$$

Y'_0 and Y_0 are respectively the rotation and the pile deflection measured at the ground surface,

3. Double differentiation of the fitting function of the bending moment M(z) to determine the soil lateral reaction profiles P(z) as follows:

$$\boldsymbol{P(z) = \frac{d^2M(z)}{dz^2}} \quad \textbf{(21)}$$

Interpretation of the experimental data for each test pile test led to the construction of the P-Y reaction curves at various depths along the pile. Fig. 8 illustrates a typical set of experimental P-Y curves (Laouedj, 2018), where it can be stated an inherent non linearity of the curve shape, and an increase in the initial stiffness of the curves with depth. Moreover, beyond a displacement of 4% of B, it can be seen the appearance of a horizontal asymptote of soil reaction, which may be interpreted by the mobilization of all the lateral soil resistance.

As depicted in Fig. 3, the P-Y curve may be well described by a hyperbolic function as follows:

$$\boldsymbol{P(z) = \frac{Y(z)}{\frac{|Y(z)|}{P_u(z)} + \frac{1}{E_{s0}(z)}}} \quad \textbf{(22)}$$

For each test pile, the experimental P-Y curves were fitted by this hyperbolic function, which led to derive the parameters E_{s0} and P_u as functions of depth z and formulate them as follows:

$$E_{s0}(z) = K_{E3}.N_{spt}(z).\ \sigma'_v(z) \tag{23}$$

$$P_u(z) = K_{N2}.B.\ \sigma'_v(z) \tag{24}$$

Table 1 – Summary of the of the experimental pile/soil system features.

Site	Location	Soil description	B (m)	D/B	E_pI_p (MN.m^2)	GWT (m)	Reference
S_1	California (USA)	Sand (SM- SC)	0.6 0.4 1.2 1.2	20.0 11.3 10.0 10.0	238 40 3530 3530	No.	Juirnarongrit & Ashford (2001)
S_2	Treasure Island (USA)	Sand (SP-SM)	0.32 0.3	35.5 38.5	28.6 37.8	0.50	Ashford & Rollins (2002)
S_3	Treasure Island (USA)	Sand (SP-SM)	0.6	23.0	291.8	0.30	Ashford & Rollins (2002)
S_4	Treasure Island (USA)	Sand (SP-SM)	0.9	16.4	1019.4	0.10	Ashford & Rollins (2002)
S_5	Taipao (Taiwan)	Multi-layered: Sand (SM)/ Silt (ML)/ Sand (SM)	0.8	40.0	790	0.00	Chiou et al. (2008)
S_6	New Zealand	Silty sand	0.45 0.45	15.0 15.0	110.6 110.6	1.00	Jennings et al. (1985)
S_7	Mustang Island, Texas (USA)	Deep layer of sand	0.61	34.5	168.4	0.00	Reese et al. (1974)
S_8	North Carolina (USA)	Multi-layered: Silty Sand / Weathered rock	0.27 0.27	20.4 20.4	21.13 21.13	No.	Brian Anderson et al. (2011)
S_9	Salt Lake City (USA)	Multi-layered: Clay (CL)/ Silt (ML)/ Clay (CL)/ Sand (SM)	0.61	18.4	230	1.07	Rollins et al. (2003)

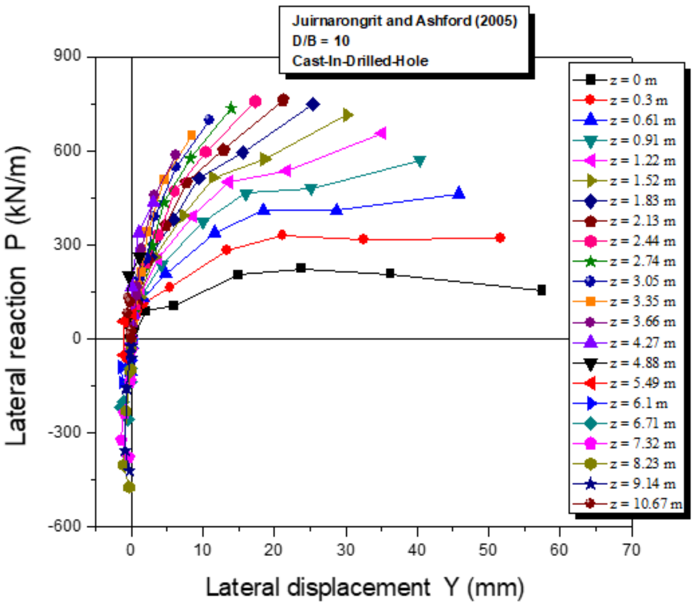

Fig. 8 Typical set of P-Y curves (Laouedj, 2018)

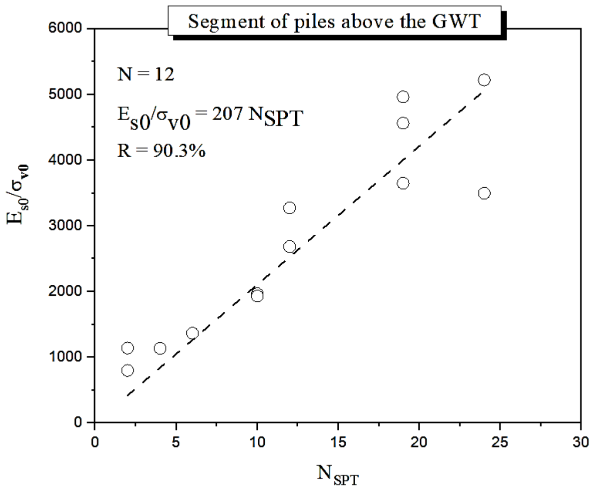

Fig. 9 Determination of the modulus number K_{E3}

3.3. Presentation and discussion of results

Synthesis of the values of factors K_{N2} and K_{E3} of all the test piles showed their dependence on the depth of P-Y curve with respect to the groundwater table (GWT). As illustrated in Fig. 9, all the points of the ratio $E_{s0}(z)/\sigma_v'(z)$ above the water table may be fitted by a linear function, giving so the modulus number K_{E3}. In table 2 are summarized the values of K_{E3}.

Moreover, the values of the factor of lateral resistance K_N were found varying very slightly with the N_{spt} value, and a statistical analysis of these values led, as shown in Fig. 10, illustrating a histogram of K_N below the water table fitted by a Gauss's probability function, led to a mean value of 17. Similarly, P-Y curves above the water table are characterized by K_N equal to 21.

Within the margin 10-40 of the slenderness ratio D/B of the test piles analysed in this study, it was found this ratio has a negligible effect on the parameters K_E and K_N.

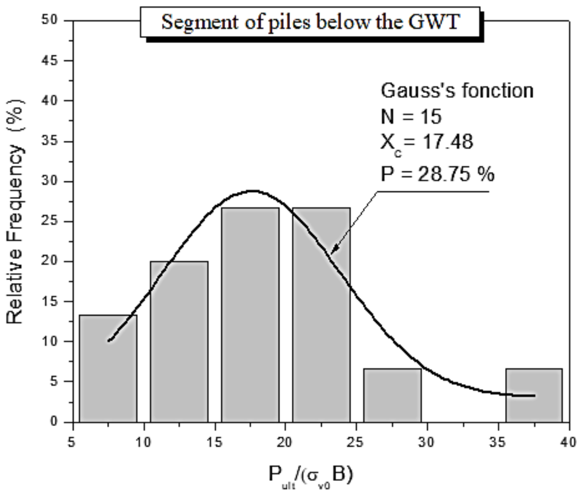

Fig. 10 Example of histogram of K_{N2} below GWT

As it can be seen in Table 2, the presence of water table leads to a non-negligible reduction of K_E and hence the lateral reaction modulus E_{s0}, by 24.6%. According to the literature, a rising water table may cause a decrease of 33–41% according to Terzaghi (1955), and 21–44% according to Reese et al (1974), which is in reasonable agreement with the value found in this study.

Similarly, due to the presence of a water table, the coefficient K_N exhibits a decrease by 19%, which means that the limit lateral resistance P_u in sand decreases due to a rising water table.

Finally, it should be noted that the N_{spt} value refers to the measured value of the blow counts during the SPT test, because no mention was made in the references of the lateral tests to the $(N_{SPT}{}^1)_{60}$ value, corresponding to the normalized and corrected measured values de N_{spt}, commonly used in geotechnical design.

It should be noted that test piles, used to develop the proposed method, are characterized by an embedded length D greater than 3 times the elastic length L_0, which correspond according to the theory of beams on elastic foundations to long flexible piles, which limits the applicability of the proposed method to the category of flexible piles (that is to say D> $3L_0$).

The lateral pile/soil stiffness ratio denoted by K_R is defined as follows:

$$\boldsymbol{K_R = \frac{E_p I_p}{E_c D^4}} \tag{25}$$

Table 2 – Values of K_{E3} and K_{N2} for flexible piles.

Above GWT	Below GWT
$K_{E3} = 207$	$K_{E3} = 156$
$K_{N2} = 21$	$K_{N2} = 17$

E_c is defined as the weighted average along an effective embedded length of the pile D_e as follows:

$$\boldsymbol{E_c = \frac{1}{D_e} \int_0^{D_e} N_{spt}(z)\sigma_{v0}(z)dz} \tag{26}$$

D_e is the "*effective length of the pile*", which is the length of the pile beyond which the pile segments do not deform. The effective length D_e is defined as the smaller of the two following quantities given by:

$$\boldsymbol{D_e = min\{D, 3L_0\}} \tag{27}$$

L_0 is the elastic length (or the transfer length) defined by:

$$\boldsymbol{L_0 = \sqrt[4]{\frac{4E_p I_p}{E_{ti}^c}}} \tag{28}$$

E_{ti}^c is called "*Characteristic lateral reaction modulus*" (or the average lateral reaction modulus) of the "*equivalent homogeneous soil*" given by:

$$\boldsymbol{E_{ti}^c = \frac{1}{D_e} \int_0^{D_e} E_{ti}(z)dz = K_E E_c} \tag{29}$$

According to the theory of beams on elastic foundations, a laterally loaded single pile behaves as a flexible pile if D > 3L0, as a rigid one if D< L0/2, and exhibits an intermediate behaviour if D is ranged between 0.5 and 3 times L0.

By combining equations (25), (26) and (29), it can easily be demonstrated that the condition D> $3L_0$ is equivalent to K_R< 0.55.

3.4. Methodology of construction of the P-Y curves

A step-by-step procedure is suggested herein to construct the P-Y curves as follows:

1. Along the pile, subdivide the soil into N horizontal slices, so thin that the NSPT values may be considered as varying linearly within any slice.
2. Assume the effective embedded length of the pile D_e=D.
3. Along the pile, compute the characteristic soil modulus EC defined by equation (26). For practical purposes, the calculation of the integral can be replaced by the approximate summation of the trapezes method.
4. Compute the lateral pile/soil stiffness ratio KR by the equation (25).
5. Determine the modulus number KiE of each layer i, from Table 2, depending on the position of the pile segment with respect to the groundwater level.
6. Compute the characteristic initial lateral modulus E_{ti}^c by equation (29).
7. Compute the elastic length L0 by the equation (28).

8. Compute D_e by equation (27). If $D > 3L_0$ (flexible pile), then repeat the steps 3 to 8 according to an iterative process introducing at each iteration the value of D_e until the process converges. Otherwise, $D < 3L_0$ the pile is rather non-flexible and the method is not applicable.
9. Compute the values of E_{s0} and Pu for each slice along the pile according to equations (23), (24) respectively, and table 2.
10. Construct the P-Y curve point-by-point by using the equation (22).
11. Use any software of analysis of single pile under lateral forces, on the basis of the suggested P-Y curves, like SPULL (Single Pile Under Lateral Loads) developed at the University of Blida.

3.5. Validation of the proposed method

The predictive capability of the proposed method was evaluated by predicting the lateral response of some simply-instrumented piles in sandy soils reported in the geotechnical literature. A total of 34 well-documented lateral full-scale loading tests carried out in 10 sandy sites worldwide were used in this regard. Detailed description of these tests may be found in Laouedj and Bouafia (2017; 2021) and Laouedj (2018). All the test piles are characterized by a stiffness ratio KR less than 10-1 and a margin of ratio D/B of 10–60, which corresponds to flexible piles.

For each test pile, the P-Y curves parameters were defined according to the methodology described above based on the SPT N-value, and a load-deflection curve was simulated by computation using SPULL.

If the ratio Y_0^{pred}/ Y_0^{meas} is considered as a random variable, it is possible to undertake a statistical analysis of the 258 values of this ratio. The histogram of this ratio, as shown in Fig. 11, was fitted by a Gaussian function, which led to a mean value μ of the ratio predicted deflection to the measured one equal to 1.25 and a standard deviation σ equal 0.44, with a probability Prob(μ) equal to 43%. It can be concluded that the P-Y curves method, based on the SPT test, estimates by a slight excess the pile head deflections, which is a pessimistic analysis but on the safe side.

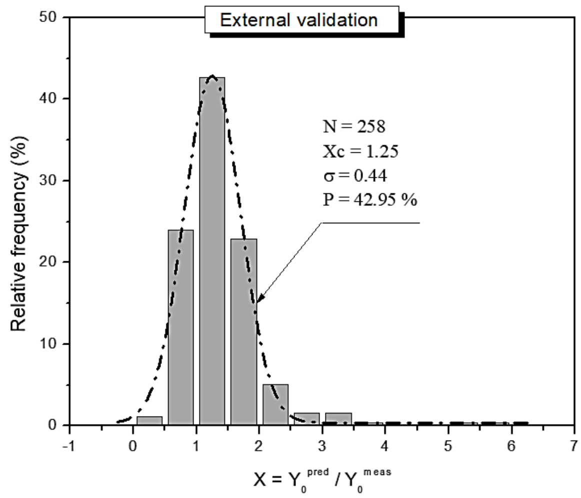

Fig. 11 Histogram of the ratio Y_0^{pred}/Y_0^{meas}

4. Conclusion

This paper presents two practical methods of defining the load-transfer functions (curves t-z, q-z curves for axial loading and P-Y curves for lateral response) to be used for the analysis of single piles in sand, on the basis of the standard penetration test SPT.

The analysis of well documented case histories of full-scale axial or lateral loading tests on single piles in sand allowed deriving the parameters of the load-transfer function in correlation with the N_{spt} value provided by the SPT test.

The two proposed methods of construction of load-transfer curves were successfully validated by predicting the displacement of test piles in sandy soils, where the comparison of the predicted pile displacements to the measured ones showed excellent predictive capability for the axial load, and a reasonable and rather pessimistic prediction for the lateral load.

References

AFNOR. (1992). *DTU-13.2: Fondations profondes pour le bâtiment* (Standard P11-212). AFNOR.

AFNOR. (2012). *Justification des ouvrages géotechniques: Norme nationale d'application de l'Eurocode 7 - Fondations profondes* (French Standard NF P94-262). AFNOR.

Ashford, S. A., & Rollins, K. M. (2002). *TILT: The Treasure Island Liquefaction Test* (No. UCSD/SSRP-2001/17). University of California, San Diego. Dept. of Structural Engineering.

ASTM. (1994). *ASTM D1143-81: Standard Test Method for Piles Under Static Axial Compressive Load*. ASTM International.

Baguelin, F., Jézéquel, J.F., & Shields, D. H. (1978). *The pressuremeter and foundation engineering* (Series on rock and soil mechanics, Vol. 2, No. 4, 1st ed.). Trans Tech Publications.

Bouafia, A. (2007). Single piles under horizontal loads: Determination of the P-Y curves from the prebored pressuremeter. *International Journal of Geotechnical and Geological Engineering*, 25, 283-301. https://doi.org/10.1007/s10706-006-9110-7

Bouafia, A. (2023a). New P-Y curve formulation for laterally loaded single piles based on the pre-bored pressuremeter. *Arabian Journal of Geosciences*, 16(684). https://doi.org/10.1007/s12517-023-11804-4

Bouafia, A. (2023b). Design of laterally loaded single piles by using P-Y curves and the cone penetration test in sandy soils. *Jordan Journal of Civil Engineering*, 17(2), 219-230. https://doi.org/10.14525/JJCE.v17i2.05

Bouafia, A. (2023c). Contribution of the standard penetration test SPT to the design of pile foundations in sand: Practical recommendations. *Journal of Engineering Research*, 11(3A), 100-111. https://doi.org/10.36909/jer.18763

Bouafia, A., & Derbala, A. (2002). Analyse de la capacité portante de cinquante pieux forés dans le sable. *Bulletin des Laboratoires des Ponts & Chaussées LCPC*, (241), 3-12.

Bowles, J. E. (1977). *Foundation analysis & design* (5th ed.). McGraw-Hill Inc.

Brian Anderson, J., & Babalola, M. R. (2011). Lateral Load Testing Micropiles to Evaluate the Impact of Threaded Joints and Casing Embedment on Short Micropiles in Shallow Rock. *DFI Journal - The Journal of the Deep Foundations Institute*, *5*(2), 23–34. https://doi.org/10.1179/dfi.2011.009

Briaud, J. L., & Tucker, L. (1984). Piles in sand: A method including residual stresses. *Journal of Geotechnical Engineering*, 110(11), 1666-1680. https://doi.org/10.1061/(ASCE)0733-9410(1984)110:11(1666)

Briaud, J.L. (2023). *Geotechnical engineering: Unsaturated and saturated soils* (2nd ed.). John Wiley & Sons.

CGS. (2006). *Canadian Foundation Engineering Manual* (4th ed.). Canadian Geotechnical Society.

Chiou, J. S., Chen, C. H., & Chen, Y. C. (2008). Deducing pile responses and soil reactions from inclinometer data of a lateral load test. *Soils and Foundations*, 48(5), 609–620. https://doi.org/10.3208/sandf.48.609

das NEVES, M., MESTAT, P., Frank, R., & DEGNY, É. (2001). Étude du comportement de pieux forés I. Expérimentations in situ et en laboratoire. *Bulletin des laboratoires des ponts et chaussées*, *231*, 55-67.

Fellenius, B. H. (2014). Response to load for four different bored piles. In *Proceedings of the DFI-EFFC International Conference on Piling and Deep Foundations* (pp. 99-120). Stockholm.

Frank, R., & Zhao, S.R. (1982). Estimation par les paramètres pressiométriques de l'enfoncement sous charges axiales de pieux forés. *Bulletin de liaison des LPC*, (119), 17-24.

Horiuchi, T., & Kani, Y. (1998). Deformation modulus of soil at the tip of a bored pile. In *Proceedings of the 4th International Conference on Case Histories in Geotechnical Engineering* (Paper No. 1-50). St. Louis, MO.

Huang, A.B., Hsueh, C., O'Neill, M., & Chen, C. (2001). Effect of construction on laterally loaded pile groups. *Journal of Geotechnical and Geoenvironmental Engineering*, 125(5), 385-397.

Jennings, D. N., Thurston, S. J., & Edmonds, F. D. (1985). Static and dynamic lateral loading of two piles. In *Proceedings of the 8th World Conference on Earthquake Engineering* (Vol. 3, pp. 561-568). San Francisco, CA.

Juirnarongrit, T., & Ashford, S. A. (2001). *Effect of pile diameter on the modulus of subgrade reaction modulus* (Report No. SSRP–2001/22). University of California.

Laouedj, A. (2018). *Apport de l'essai spt au dimensionnement des pieux isolés sous charge latérale monotone-analyse expérimentale et numérique des courbes de réaction PY* (Doctoral dissertation, Universite Mouloud Mammeri).

Laouedj, A., & Bouafia, A. (2017). Pieux isolés sous charges latérales: Construction des courbes P-Y à partir de l'essai SPT. *Revue Française de Géotechnique*, (152), 4. https://doi.org/10.1051/geotech/2017016

Laouedj, A., & Bouafia, A. (2021). P-Y curves for single piles in sand from the standard penetration test (SPT). *Journal of Materials & Engineering Structures (JMES)*, 8(1), 159-172. http://revue.ummto.dz/index.php/JMES/article/view/2338

Ménard, L., Bourdon, G., & Gambin, M. (1971). Méthode générale de calcul d'un rideau ou d'un pieu sollicité horizontalement en fonction des résultats pressiométriques. *Journal Sols/Soils*, 6(22/23), 16-29.
Mosher, R. L., & Dawkins, W. P. (2000). *Theoretical manual for pile foundations* (Report ERDC/ITL). US Army Corps of Engineers.
PHRI. (1980). *TSPHF: Technical standards for port & harbour facilities in Japan* (Chapter 4: Bearing capacity of pile foundation, pp. 123-136).
Poulos, H., & Davis, H. (1980). *Pile foundation analysis & design* (Series in Geotechnical Engineering). New York : Wiley.
Reese, L. C., Cox, W. R., & Koop, F. D. (1974). Analysis of laterally loaded piles in sand. In *Proceedings of the 6th Offshore Technology Conference* (pp. 473-483). Houston, TX. https://doi.org/10.4043/2080-MS
Rollins, K. M., Olsen, R. J., Egbert, J. J., Olsen, K. J., Jensen, D. H., & Garrett, B. H. (2003). *Response, analysis, and design of pile groups subjected to static and dynamic lateral loads* (Report No. UT-03.03). Utah. Brigham Young University. Department of Civil and Environmental Engineering.
Terzaghi, K. (1955). Evaluation of coefficients of subgrade modulus. *Géotechnique*, 5(4), 297-326. https://doi.org/10.1680/geot.1955.5.4.297
Verbrugge, J. C. (1981). Évaluation du tassement des pieux à partir de l'essai de pénétration statique. *Revue Française de Géotechnique*, (15), 75-82.
Yaich-achour, N. (2004). *Paramètres de transfert de charges: Modélisation numérique et analyse d'une base de données* [M.Sc Thesis, University of Blida].